5016 *Biochemistry* **2010,** *49,* 5016–5027
DOI: 10.1021/bi100502z

BIOCHEMISTRY
including biophysical chemistry & molecular biology
Article

Kinetic and Structural Characterization of a Heterohexamer 4-Oxalocrotonate Tautomerase from *Chloroflexus aurantiacus* J-10-fl: Implications for Functional and Structural Diversity in the Tautomerase Superfamily[†,‡]

Elizabeth A. Burks,[§] Christopher D. Fleming,[∥] Andrew D. Mesecar,[∥] Christian P. Whitman,*[,§] and Scott D. Pegan*[,∥,⊥]

[§]*Division of Medicinal Chemistry, College of Pharmacy, The University of Texas, Austin, Texas 78712,* [∥]*Center for Pharmaceutical Biotechnology (MC 870), College of Pharmacy, University of Illinois, 900 South Ashland Avenue, Chicago, Illinois 60607-7173, and* [⊥]*Department of Chemistry and Biochemistry, University of Denver, Denver, Colorado 80208-0183*

Received April 2, 2010; Revised Manuscript Received May 12, 2010

ABSTRACT: 4-Oxalocrotonate tautomerase (4-OT) isozymes play prominent roles in the bacterial utilization of aromatic hydrocarbons as sole carbon sources. These enzymes catalyze the conversion of 2-hydroxy-2,4-hexadienedioate (or 2-hydroxymuconate) to 2-oxo-3-hexenedioate, where Pro-1 functions as a general base and shuttles a proton from the 2-hydroxyl group of the substrate to the C-5 position of the product. 4-OT, a homohexamer from *Pseudomonas putida* mt-2, is the most extensively studied 4-OT isozyme and the founding member of the tautomerase superfamily. A search of five thermophilic bacterial genomes identified a coded amino acid sequence in each that had been annotated as a tautomerase-like protein but lacked Pro-1. However, a nearby sequence has Pro-1, but the sequence is not annotated as a tautomerase-like protein. To characterize this group of proteins, two genes from *Chloroflexus aurantiacus* J-10-fl were cloned, and the corresponding proteins were expressed. Kinetic, biochemical, and X-ray structural analyses show that the two expressed proteins form a functional heterohexamer 4-OT (hh4-OT), composed of three $\alpha\beta$ dimers. Like the *P. putida* enzyme, hh4-OT requires the amino-terminal proline and two arginines for the conversion of 2-hydroxymuconate to the product, implicating an analogous mechanism. In contrast to 4-OT, hh4-OT does not exhibit the low-level activity of another tautomerase superfamily member, the heterohexamer *trans*-3-chloroacrylic acid dehalogenase (CaaD). Characterization of hh4-OT enables functional assignment of the related enzymes, highlights the diverse ways the $\beta-\alpha-\beta$ building block can be assembled into an active enzyme, and provides further insight into the molecular basis of the low-level CaaD activity in 4-OT.

4-Oxalocrotonate tautomerase (4-OT),[1] initially cloned from the TOL plasmid pWW0 in *Pseudomonas putida* mt-2, catalyzes the conversion of 2-hydroxy-2,4-hexadienedioate, known more commonly as 2-hydroxymuconate [**1** (Scheme 1)] to 2-oxo-3-hexenedioate (**2**) (*1*−*5*). The enzyme is part of the meta-fission pathway, which is a catabolic pathway for aromatic hydrocarbons. Organisms having the TOL plasmid can process simple aromatic hydrocarbons (e.g., benzene, toluene, *m*- and *p*-xylene, 3-ethyltoluene, and 1,2,4-trimethylbenzene) as their sole sources of carbon and energy (*3*).

4-OT is a member of the tautomerase superfamily, which is a group of structurally homologous proteins, characterized by a $\beta-\alpha-\beta$ scaffold and a catalytic amino-terminal proline (*6*−*11*). There are five known families of this superfamily represented by the key members, 4-OT, 5-(carboxymethyl)-2-hydroxymuconate isomerase (CHMI), macrophage migration inhibitory factor (MIF) (*7*, *8*), *cis*-3-chloroacrylic acid dehalogenase (*cis*-CaaD) (*9*), and malonate semialdehyde decarboxylase (MSAD) (*10*). The 4-OT family includes *trans*-3-chloroacrylic acid dehalogenase (CaaD). Superfamily members have been described as trimers (CHMI, MIF, *cis*-CaaD, and MSAD), a heterohexamer (CaaD), a homodimer (a 4-OT homologue designated YdcE) (*11*), and homohexamers (4-OT and a 4-OT homologue designated YwhB) (*7*, *8*). These enzymes mediate tautomerization, dehalogenation, hydration, and decarboxylation reactions. Thus far, Pro-1 is a critical residue for the activities of all of these enzymes.

During the course of a search for other superfamily members, the genomes of five recently sequenced thermophilic organisms exhibited an intriguing peculiarity: each had a protein annotated

[†]This research was supported by National Institutes of Health (NIH) Grants GM-41239 (C.P.W.) and AI-60915 (S.D.P.), Robert A. Welch Foundation Grant F-1334 (C.P.W.), and U.S. Department of Defense Grant W81XWH0710445 USAMRAA (S.D.P.). Use of the Advanced Photon Source is supported by the U.S. Department of Energy, Office of Science, Office of Basic Energy Sciences, under Contract W-31-109-Eng-38. The Analytical Instrumentation Facility Core (College of Pharmacy, The University of Texas) is supported by NIH Center Grant ES07784.

[‡]The atomic coordinates and structure factors have been deposited with the Brookhaven Protein Data Bank (entry 3MB2).

*To whom correspondence should be addressed. C.P.W.: telephone, (512) 471-6198; fax, (512) 232-2606; e-mail, whitman@mail.utexas.edu. S.D.P.: telephone, (303) 871-2533; fax, (303) 871-2254; e-mail, scott.pegan@du.edu.

[1]Abbreviations: Ap, ampicillin; BSA, bovine serum albumin; dNTPs, deoxyribose nucleotide triphosphates; CHMI, 5-(carboxymethyl)-2-hydroxymuconate isomerase; CaaD, *trans*-3-chloroacrylic acid dehalogenase; *cis*-CaaD, *cis*-3-chloroacrylic acid dehalogenase; DSC, differential scanning calorimetry; HEPES, *N*-(2-hydroxyethyl)piperazine-*N*′-2-ethanesulfonate; hh4-OT, heterohexamer 4-oxalocrotonate tautomerase; IPTG, isopropyl β-D-thiogalactoside; Kn, kanamycin; LB, Luria-Bertani; MIF, macrophage migration inhibitory factor; MSAD, malonate semialdehyde decarboxylase; NCBI, National Center for Biotechnology Information; NMR, nuclear magnetic resonance; 4-OT, 4-oxalocrotonate tautomerase; PEG, polyethylene glycol; PPT, phenylpyruvate tautomerase; PCR, polymerase chain reaction; rmsd, root-mean-square deviation; SDS−PAGE, sodium dodecyl sulfate−polyacrylamide gel electrophoresis.

 Published on Web 05/13/2010

Scheme 1

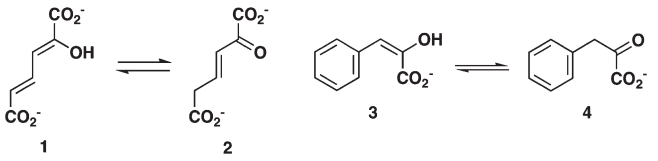

as a 4-OT homologue in what appeared to be a catabolic pathway for aromatic hydrocarbons, but the homologue lacked Pro-1.[2] Moreover, each organism had a second protein of similar length in the vicinity of the hypothetical tautomerase with the amino-terminal proline, but these sequences were not annotated as tautomerase-like. Because it was not immediately obvious what role these two proteins might play, the corresponding genes were cloned from *Chloroflexus aurantiacus* J-10-fl, and the two proteins were produced and characterized. The proteins form an $\alpha\beta$ dimer, and the active tautomerase is a heterohexamer, which converts **1** to **2**, and phenylenolpyruvate [**3** (Scheme 1)] to phenylpyruvate (**4**). Mutagenesis analysis implicates βPro-1, αArg-12, and αArg-40 as critical residues for these activities, whereas βArg-11 and βArg-39 are not required for activity. A crystal structure confirms the heterohexamer arrangement and shows that the active site contains βPro-1, αArg-12, and αArg-40. Despite the mechanistic parallels and active site similarities, hh4-OT lacks a significant property of 4-OT; it does not have a low-level CaaD activity. This is the first reported 4-OT heterohexamer, and its properties have implications for the evolution of other superfamily members.

EXPERIMENTAL PROCEDURES

Materials. Chemicals, biochemicals, buffers, and solvents were purchased from Sigma-Aldrich Chemical Co. (St. Louis, MO), Fisher Scientific Inc. (Pittsburgh, PA), Fluka Chemical Corp. (Milwaukee, WI), or EM Science (Cincinnati, OH). The Centricon and Ultrafree centrifugal filter devices were obtained from Millipore Co. (Billerica, MA). The synthesis of 2-hydroxymuconate (**1**) is reported elsewhere (*4*). Recombinant 4-OT, cloned from the TOL plasmid of *P. putida* mt-2 and expressed in *Escherichia coli* strain BL21-Gold(DE3), was purified by modifying previously reported procedures (*13*, *14*), as reported in the Supporting Information. The Phenyl Sepharose 6 Fast Flow and the Sephacryl-S100 High Resolution resins were obtained from GE Healthcare (Piscataway, NJ). The Econo-Column chromatography columns and Freeze 'N Squeeze units, used for extraction of DNA from agarose gels, were obtained from Bio-Rad Laboratories, Inc. (Hercules, CA). Enzymes and reagents used for molecular biology procedures were obtained from New England Biolabs, Inc. (Ipswich, MA). The sources for the components of Luria-Bertani (LB) medium have been reported elsewhere (*15*).

Bacterial Strains, Plasmids, and Growth Conditions. *C. aurantiacus* J-10-fl was provided by M. T. Madigan (*16*). Cells of the strain were grown at 50 °C under a tungsten light as described elsewhere (*16*). The cells were stored at −80 °C until they were ready for use. *E. coli* strain DH5α was obtained from Invitrogen (Carlsbad, CA). *E. coli* strain BL21-Gold(DE3) and pBluescript II SK$^-$ were obtained from Stratagene (La Jolla, CA). The pET vectors were obtained from Novagen (Madison, WI).

General Methods. Techniques for restriction enzyme digestion, ligation, transformation, and other standard molecular biology manipulations were based on methods described elsewhere (*15*). Oligonucleotide primers were synthesized by Invitrogen. DNA sequencing was performed at the DNA core facility of the Institute for Cellular and Molecular Biology at The University of Texas. Mass spectral data were obtained on an LCQ electrospray ion-trap mass spectrometer (Thermo, San Jose, CA) in the Analytical Instrumentation Facility Core in the College of Pharmacy at The University of Texas. Samples were prepared as described elsewhere (*17*). Kinetic data were obtained at 24 °C on an Agilent 8453 diode-array spectrophotometer. Nonlinear regression data analysis was performed using Grafit (Erithacus Software Ltd., Staines, U.K.) obtained from Sigma-Aldrich. Plasmids were isolated from cell cultures using the QIAprep Miniprep Kit (Qiagen, Valencia, CA). Protein concentrations were determined by the method described by Waddell (*18*). Protein was analyzed by tricine sodium dodecyl sulfate−polyacrylamide gel electrophoresis (SDS−PAGE) on 15% T/2% C gels on a vertical gel electrophoresis apparatus obtained from Idea Scientific (Minneapolis, MN) (*19*). BLAST and iterative PSI-BLAST searches of the National Center for Biotechnology Information (NCBI) databases were performed using the 4-OT amino acid sequence from the TOL plasmid of *P. putida* mt-2 as the query sequence (*13*). Nuclear magnetic resonance (NMR) spectra were recorded in 100% H_2O on a Varian Unity INOVA-500 spectrometer as reported previously (*17*).

Cloning of the α- and β-Subunits of hh4-OT from Genomic DNA. Genomic DNA was extracted from 50 mg of cells following a protocol described elsewhere (*20*). The coding regions for the two subunits were amplified from genomic DNA in separate PCRs.[3] Each PCR mixture (50 μL) contained genomic DNA (0.5 μg), two 5′-phosphorylated primers for blunt cloning (0.4 μM), dNTPs (0.3 mM), bovine serum albumin (BSA, 0.5 mM), Vent polymerase (0.5 unit), and the accompanying 10× buffer (diluted to 1×). For the α-subunit, the forward primer (αG1) had the sequence 5′-GGACGGTGATATGCTACTTC-3′ and the reverse primer (αG2) had the sequence 5′-GTTCTGAACAAACGAGTTAC-3′. For the β-subunit, the forward primer (βG1) had the sequence 5′-CTCCACTTACGGTTCGTGTG-3′ and the reverse primer (βG2) had the sequence 5′-CGCTTTACCCATCACCTATC-3′. The primers were designed to match the areas just upstream and downstream of the coding region of each subunit. The PCR amplification protocol consisted of an initial 5 min denaturation cycle at 94 °C, followed by 29 cycles of 94 °C for 1 min, 55 °C for 2 min, and 72 °C for 3 min, a 10 min elongation cycle at 72 °C, and ending with a hold at 4 °C. The gel-purified PCR products were each ligated into an *Eco*RV-digested pBluescript II SK$^-$. An aliquot of each ligation mixture was used to transform *E. coli* DH5α cells by electroporation. A positive colony resulting from each transformation was selected on the basis of PCR screening. The plasmid from each colony was isolated, sequenced, and designated the α- or β-genomic clone.

Construction of the Bluescript hh4-OT Dicistronic Clone. The α-subunit was amplified by PCR from the corresponding α-genomic clone using the oligonucleotide 5′-TAGTAGTAGGAATTCAAGAAGGAGATATACATATGCTACTTC-3′

[2]The initiating methionine is the first amino acid according to the gene sequence. However, proteins with a proline in the second position undergo post-translational modification to remove the initiating methionine, so that proline becomes the amino-terminal amino acid (*12*).

[3]The sequence of the genomic DNA was obtained from the NCBI website (accession number NC_010175). The protein accession numbers are YP_001634971 (gi|163846927) for the α-subunit (which appears first in the genome) and YP_001634975 (gi|163846931) for the β-subunit.

as the forward primer and the αG2 primer (above) as the reverse primer. The forward primer contains nine nonspecific bases (to enhance restriction enzyme digestion efficiency), a ribosome binding site, an *Nde*I restriction site (underlined), and seven additional gene-specific bases. The PCR mixture (50 μL) contained the α-genomic clone (12 ng of plasmid), primers (0.2 μM), dNTPs (0.2 mM), BSA, (0.5 mM), Vent polymerase (0.5 unit), and the accompanying 10× buffer (diluted to 1×). The PCR amplification protocol consisted of an initial 2 min denaturation cycle at 94 °C, followed by 29 cycles of 94 °C for 1 min, 55 °C for 2 min, and 72 °C for 3 min, and ended with a 10 min elongation cycle at 72 °C, followed by a hold at 4 °C. The gel-purified product was phosphorylated and blunt cloned into pBluescript II SK$^-$ at the *Eco*RV site. The resulting clone lacked the first 16 bases of the forward primer and had the α-subunit oriented such that an *Eco*RI site of the vector was at the 3′-end of the gene.

The β-subunit was amplified by the PCR from the β-genomic clone using the oligonucleotides 5′-TAGTAGTAGGAATTCAAGAAGGAGATATA*CATATG*CCGATGC-3′ and 5′-GATGATGATCTCGAG*GGATCC*TCATTATTACTGCTGGTCTGGC-3′ as the forward and reverse primers, respectively. The forward primer contains nine nonspecific bases, an *Eco*RI restriction site (underlined), a ribosome binding site, an *Nde*I restriction site (italicized), and seven gene-specific bases. The reverse primer contains nine nonspecific bases, an *Xho*I restriction site (underlined), a *Bam*HI restriction site (italicized), three stop codons, and 10 gene-specific bases. The PCR mixture (100 μL) contained the β-genomic clone (1 μL of gel extract), the primers (0.2 μM), dNTPs (0.2 mM), Vent polymerase (1 unit), and the accompanying 10× buffer (diluted to 1×). Two separate reactions were conducted using a PCR amplification protocol that consisted of an initial 2 min denaturation cycle at 94 °C, followed by 25 cycles of 94 °C for 45 s, 55 °C for 45 s, and 72 °C for 2 min, and ended with a 10 min elongation cycle at 72 °C, followed by a hold at 4 °C.

The product was cloned into the pBluescript construct containing the α-subunit between the *Eco*RI and *Bam*HI restriction sites as follows. The gel-purified PCR product and the pBluescript construct containing the α-subunit were treated with *Eco*RI and *Bam*HI restriction enzymes, purified, and ligated using T4 DNA ligase. Aliquots of the ligation mixture were used to transform competent *E. coli* DH5α cells. Transformants were selected at 37 °C on LB/Ap (100 μg/mL) plates. The plasmid was isolated from one clone, sequenced, and used for the production of hh4-OT.

Cloning of the Dicistronic Gene for hh4-OT into pET24a. The dicistronic gene for hh4-OT was amplified from the pBluescript construct (containing the dicistronic gene) by the PCR using the forward primer 5′-TAGTAGTAGTCTAGAGGTATCGATAAGCTTG-3′ and the reverse primer 5′-GATGATGATCTCGAGACTAGTGGATCC-3′. The forward primer contains nine nonspecific bases (for restriction enzyme digestion efficiency), an *Xba*I restriction site (underlined), and 16 bases specific for the 5′ area upstream of the dicistronic gene in the pBluescript construct. The reverse primer contains nine nonspecific bases (for restriction site digestion efficiency), an *Xho*I restriction site (underlined), and 12 bases specific for the 3′ area downstream of the dicistronic gene in the pBluescript construct. The PCR mixture (200 μL) contained the pBluescript construct (160 ng), the primers (0.5 μM), dNTPs (0.2 mM), Taq polymerase (6 units), and the accompanying 10× buffer (diluted to 1×). The PCR amplification protocol consisted of an initial 2 min denaturation cycle at 94 °C, followed by 29 cycles of 94 °C for 1 min, 55 °C for 2 min, and 72 °C for 3 min, and ended with a 10 min elongation cycle at 72 °C, followed by a hold at 4 °C. The gel-purified PCR product and the pET24a vector were treated with *Xba*I and *Xho*I restriction enzymes, purified, and ligated using T4 DNA ligase. Aliquots of the ligation mixture were used to transform competent *E. coli* DH5α cells. Transformants were selected at 37 °C on LB/Kn (30 μg/mL) plates. Two colonies were randomly chosen for sequencing. Both clones showed the correct sequences for the α- and β-dicistronic gene arrangement. Plasmid DNA was isolated from one clone and used as the expression vector in *E. coli* BL21-Gold(DE3) cells.

Expression and Purification of hh4-OT and Construction, Expression, and Purification of the hh4-OT Mutants. The expression, overproduction, and purification protocols for the hh4-OT are provided in the Supporting Information. The experimental procedures used for the construction, expression, overproduction, purification, and mass spectral analysis of the hh4-OT mutants are also provided in the Supporting Information.

Enzyme Assays and Kinetic Studies. The tautomerization activities of hh4-OT were measured by monitoring the ketonization of **1** to **2** and **3** to **4** in 10 mM potassium phosphate buffer (pH 7.3) at 24 °C (*4*, *5*). Stock solutions (20 mM) of 2-hydroxymuconate (**1**) and phenylenolpyruvate (**3**) were made up in ethanol and diluted (with ethanol) to 10 mM. The ketonization of **1** to **2** was assessed by following the increase in absorbance at 236 nm (ε = 6580 M^{-1} cm^{-1}) using substrate concentrations ranging from 10 to 200 μM (*4*). The ketonization of **3** to **4** was assessed by following the decrease in absorbance at 283 nm (ε = 18000 M^{-1} cm^{-1}) using substrate concentrations ranging from 10 to 140 μM (*5*). An aliquot of enzyme was diluted into the potassium phosphate buffer, yielding a final dimer concentration of 1−191 nM for reactions using **1** and 100−1000 nM for reactions using **3**. Reactions were initiated by the addition of substrate.

The spectrophotometric assay used to monitor the dehalogenation of *trans*- or *cis*-3-chloroacrylic acid was modified from previously reported protocols (*17*, *21*). Accordingly, reaction mixtures containing 10 mM potassium phosphate buffer (pH 7.3), substrate [*trans*- or *cis*-3-chloroacrylic acid (0.5 mM)], and enzyme (wild type, βR11A mutant, and βR39A mutant) were incubated at room temperature. An aliquot of enzyme was diluted into the potassium phosphate buffer, yielding final dimer concentrations of 4.5, 5.0, and 4.9 μM for the wild-type, βR11A mutant, and βR39A mutant enzymes, respectively. After 2 weeks, there was no change in the absorbance at 224 nm.

^{1}H NMR Spectroscopic Monitoring of the Incubation Mixture Containing hh4-OT and trans-3-Chloroacrylic Acid (**5**). The ^{1}H NMR experiments were conducted as previously reported (*17*, *22*), with the following modifications. Accordingly, an aliquot (0.6 mL) of **5** (Scheme 2) was transferred to an NMR tube from a stock solution made up in 100 mM Na_2HPO_4 buffer. The aliquot contained 4 mg (0.04 mmol) of the substrate. DMSO-d_6 (30 μL) was also added to the tube. The pH of the reaction mixture was then adjusted to 9.3 using small amounts of an aqueous 1 M NaOH solution. Subsequently, an aliquot of hh4-OT (50 μL of a 5.6 mg/mL solution of hh4-OT) from a solution made up in 20 mM Na_2HPO_4 buffer (pH 7.3) was added to the reaction mixture. ^{1}H NMR spectra were recorded 10 days and 7 weeks after the addition of enzyme to the NMR tube. At both intervals, the enzyme was examined for hh4-OT activity using **1** and found to be active.

Scheme 2

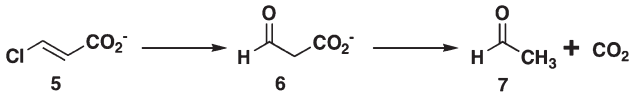

Enzymatic Activity as a Function of the Oligomer State. The construction of pET24a vectors containing individual α- and β-subunits is described in the Supporting Information. The genes were then expressed separately in *E. coli* BL21-Gold(DE3) cells, and the separate α- and β-subunits were partially purified and examined for activity (using **1**) before and after treatment with 8 M urea. Accordingly, the cells (~2−4 g each) were suspended in 20 mM HEPES buffer (~10 mL, pH 7.6). The individual suspensions were sonicated and protease inhibitors added (see the Supporting Information). The lysed cell mixtures were centrifuged for 45 min (30000*g*), followed by recovery of the supernatants, which were then centrifuged for 3 h (264000*g*). The individual supernatants (containing the α- or β-subunit) were treated with urea in separate tubes when the supernatant (0.09 mL) was mixed with urea [0.4 mL of 10 M urea in 20 mM HEPES buffer (pH 7.3)]. A small amount of NaCl [0.01 mL of 5 M NaCl in 20 mM HEPES buffer (pH 7.3)] was added to each sample. Rapid dilution was achieved by mixing an aliquot (10 μL) with 1 mL of 10 mM KH_2PO_4 buffer (pH 7.3). The sample was then assayed for activity using **1** (10 μL of a 20 mM solution of **1**). In addition to these samples, a mixture of the urea-treated α- and β-subunits (~1:1) was rapidly diluted and assayed, as described above. Each sample was examined by SDS−PAGE (15% T/2% C gels) to verify the presence of two proteins with the correct molecular masses.

Crystallization and Structural Determination of hh4-OT. The initial crystallization conditions for hh4-OT were determined from the high-throughput screening of Qiagen Nextel screens, Classics, Classics II, polyethylene glycol (PEG)s, and PEGs II suites, with a Tecan Freedom Evo 200 liquid handling robot. The hh4-OT [20 mg/mL in 10 mM Na/KPO_4 buffer (pH 7.3)] was mixed in a 1:1 ratio with precipitant to give a total volume of 2 μL in a sitting drop formatted microplate with a 100 μL reservoir solution. Final crystals for hh4-OT were obtained by the hanging drop vapor diffusion method with a 500 μL reservoir and 4 μL hanging drops that contained protein and precipitant, 0.25 M $(NH_4)_2SO_4$ and 4% PEG 4000, in a 1:1 ratio. Crystals appeared in the course of 3−5 days.

The X-ray diffraction data were collected for the hh4-OT crystals to 2.41 Å resolution at the Argonne National Laboratory (Argonne, IL) on Southeast Regional Collaborative Access Team (SER-CAT) beamline 22-BM. Crystals were mounted on nylon loops and submerged in a 4 μL drop of a cryo solution containing 0.25 M $(NH_4)_2SO_4$ and 25% PEG 4000. The crystals were then immediately flash-frozen by being submerged in liquid nitrogen. The flash-frozen crystals were mounted on a goniostat under a stream of dry N_2 at 100 K. X-ray exposures of 1 s per degree of rotation about 200° omega were collected on a MAR 225 CCD detector. The X-ray data were processed and scaled using HKL2000 (*23*). The data collection statistics are listed in Table 1.

The molecular replacement solutions were determined using PHASER (*24*). The overall search model was based on the heterohexamer CaaD [Protein Data Bank (PDB) entry 1S0Y] comprised of an α-subunit homology model produced by 3D-Jigsaw using a 4OT homologue, *Haemophilus influenzae* (PDB entry 1MWW), and a β-subunit hh4-OT homology model derived from MODELER using the *Pseudomonas* sp. CF600 4OT isozyme (PDB entry 1OTF) (*25*−*27*). WINCOOT was used for model building, and REFMAC from the CCP4 software suite was used for restrained TLS refinement using 36 TLS groups (*24*, *28*). The refinement statistics are listed in Table 1.

Table 1: Data Collection and Refinement Statistics for hh4-OT

Data Collection	
space group	$P3_1$
unit cell dimensions	
a, *b*, *c* (Å)	106.1, 106.1, 110.0
$\alpha = \beta = \gamma$ (deg)	90, 90, 120
resolution (Å)	91.85−2.41
no. of reflections observed	297700
no. of unique reflections	49737
R_{merge} (%)	7.2 (43.9)[a]
$I/\sigma(I)$	27.6 (4.1)[a]
% completeness	98.6 (88.9)[a]
Refinement	
resolution range (Å)	91.85−2.41
no. of reflections in working set	47067
no. of reflections in test set	2670
R_{work} (%)	20.0
R_{free} (%)	25.0
average *B* factor (Å^2)	32.1
protein	31.70
ions	59.60
water	32.80
rmsd	
bond lengths (Å)	0.026
bond angles (deg)	2.23
no. of protein/water atoms	5447/249

[a]Data for the last resolution shell are given in parentheses.

Differential Scanning Calorimetry. Samples of hh4-OT from *C. aurantiacus* J-10-fl and 4OT from *P. putida* mt-2 were filtered through a 0.22 μm syringe filter following overnight dialysis in 10 mM sodium phosphate buffer (pH 7.3). The protein samples were subsequently diluted using the same buffer to concentrations of 0.14 mg/mL (299 μM in heterohexamer) for hh4-OT and 0.21 mg/mL (524 μM in homohexamer) for *P. putida* mt-2 4-OT. Heat capacity measurements were taken using a VP-DSC differential scanning calorimeter (Microcal, Northampton, MA) over a temperature range of 10−125 °C under ~28 psi (1.9 atm). Samples were heated at a rate of 90 °C/h. An accurate baseline was derived from five buffer−buffer scans, which were subtracted from five scans performed on each enzyme. Heat capacity was plotted versus temperature to determine the temperature of maximal heat capacity (T_m) for both protein samples after normalization for the protein concentrations. Origin version 5.0 was used for all differential scanning calorimetry (DSC) data analysis.

RESULTS

Sequence Analysis for the hh4-OT Homologues. A sequence similarity search of the NCBI database was performed with the BLASTP program using the 4-OT amino acid sequence from the TOL plasmid of *P. putida* mt-2 as the query sequence (*13*). The search yielded a sequence from *Roseiflexus* sp. RS-1 (GenBank entry YP_001276901])that was annotated as a tautomerase-like protein but showed a leucine rather than a proline following the initiating methionine. Examination of the

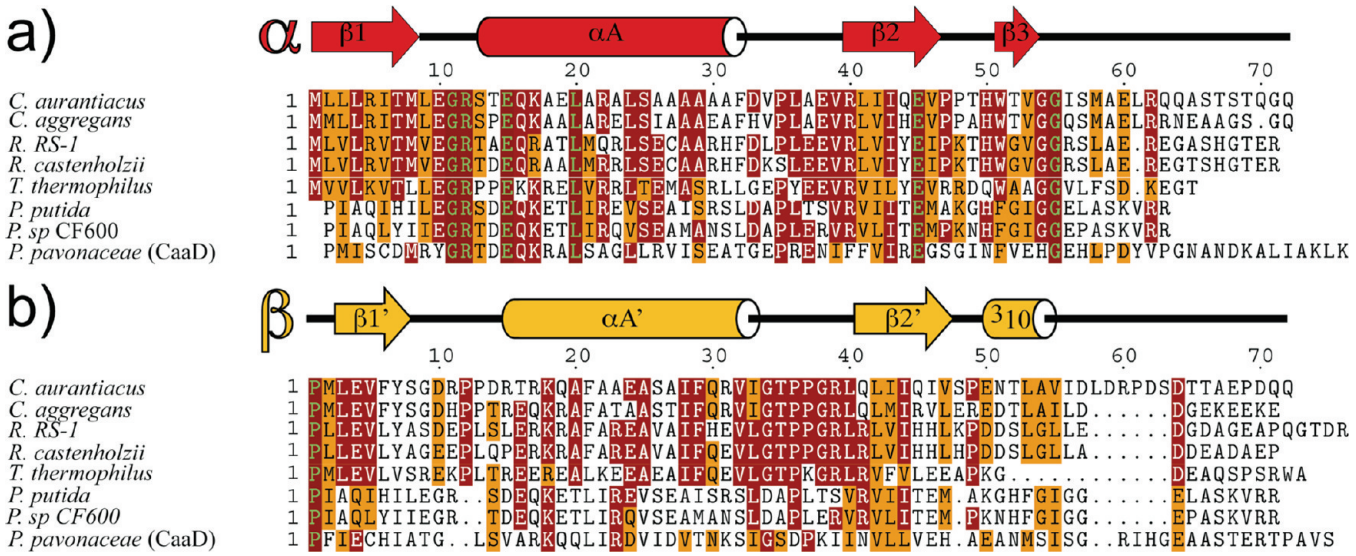

FIGURE 1: Sequence alignment of the α- and β-subunits of the thermophilic hh4-OTs along with the 4-OT isozymes from *P. putida* mt-2 and *Pseudomonas* sp. CF600 and the α- and β-subunits of CaaD (from *Pseudomonas pavonaceae*). The secondary structure elements are shown above each set and were generated by a dictionary of protein secondary structure using the *C. aurantiacus* J-10-fl hh4-OT structure (*41*). The shading indicates similar (orange), conserved (red), and absolutely conserved (red with green text) residues. (a) The sequences are ordered from the highest to lowest percentage of sequence similarity with the α-subunit of *C. aurantiacus* J-10-fl (gi|163846927) (from top to bottom). Accordingly, the α-subunit of *Chloroflexus aggregans* DSM 9485 (gi|219848927) is 59% similar, the α-subunit of *Roseiflexus* sp. RS-1 (gi|148656696) 58% similar, the α-subunit of *Roseiflexus castenholzii* DSM 13941 (gi|156742377) 57% similar, the α-subunit of the *Thermus thermophilus* HB8 plasmid (gi|55978425) 40% similar, 4-OT from *P. putida* mt-2 (gi|150974) 41% similar, 4-OT from *Pseudomonas* sp. CF600 (gi|1421033) 38% similar, and the α-subunit of CaaD from *P. pavonaceae* (gi|10637969) 29% similar. (b) The sequences are shown in the order of the highest to lowest percentage of sequence similarity with the β-subunit of *C. aurantiacus* J-10-fl (gi|163846931) (from top to bottom). Accordingly, the β-subunit of *C. aggregans* DSM 9485 (gi|219848931) is 70% similar, the β-subunit of *Roseiflexus* sp. RS-1 (gi|148656700) 51% similar, the β-subunit of *R. castenholzii* DSM 13941 (gi|156742373) 50% similar, the β-subunit of the *T. thermophilus* HB8 plasmid (gi|55978421, one asterisk) 46% similar, 4-OT from *P. putida* mt-2 13.9% similar (two asterisks), 4-OT from *Pseudomonas* sp. CF600 15.3% similar (two asterisks), and the β-subunit of *P. pavonaceae* CaaD (gi|10637970) 21% similar. Alignment and similarity calculation were obtained by using the CLUSTALW, TEXSHADE, BL2SEQ, and ALIGN programs, which can be found at http://workbench.sdsc.edu/. The BL2SEQ settings were as follows: Matrix = BLOSUM62. The CLUSTERW settings were as follows: Gap Opening Penalty = 11, Gap Extension Penalty = 1, and Lambda Ratio = 0.85. The single asterisk indicates that the reported sequence is missing the initiating methionine and proline. A review of the corresponding gene indicated that the missing amino acids are present. The double asterisk indicates that the ALIGN program was used.

genomic context for this gene (gi|148656696) using the genome project link at the NCBI website revealed the presence of the genes encoding enzymes similar to the ones surrounding 4-OT in the TOL plasmid, including 2-hydroxymuconate semialdehyde dehydrogenase (which precedes 4-OT in the meta-fission pathway) and 4-oxalocrotonate decarboxylase and vinylpyruvate hydratase (which follow 4-OT in the meta-fission pathway) (*1*−*3*). Using the *Roseiflexus* sp. RS-1 sequence as the query sequence in a BLAST search yielded several highly similar sequences (40−59% sequence similarity) that were also annotated as tautomerase-like proteins, but none had a proline following the initiating methionine (Figure 1a). Examination of the genomic context of each also showed genes encoding proteins typically associated with the meta-fission pathway as well as a hypothetical protein with approximately the same number of amino acid residues (63−73 amino acids) (Figure 1b). Examination of the sequences of each of these hypothetical proteins showed that they have a proline following the initiating methionine, but apparently, the sequences do not trigger the tautomerase designation by the BLAST domain search. This study indicated that the first set of sequences (Figure 1a) likely corresponds to the α-subunit of a hh4-OT and the second set of sequences (Figure 1b) likely corresponds to the β-subunit of a hh4-OT. The α- and β-subunits of *C. aurantiacus* J-10-fl hh4-OT are ∼44% similar and ∼22% identical in sequence.

Expression, Purification, and Characterization of hh4-OT and Its Mutants. The α- and β-subunits were initially cloned from *C. aurantiacus* J-10-fl genomic DNA and inserted individually into pBluescript expression vectors. A dicistronic gene for the hh4-OT was then constructed by cloning the β-subunit into the pBluescript vector containing the α-subunit. The five hh4-OT mutants were constructed using the dicistronic pBluescript construct. Finally, a high-expression level pET system was constructed by amplifying the dicistronic region from pBluescript (using the PCR) and inserting the construct into a pET24a vector at the *Xba*I and *Xho*I restriction sites.

The recombinant hh4-OT and the five mutants (αR12A, αR40A, βP1A, βR11A, and βR39A) were purified in a three-step protocol (heat treatment, anion exchange, and gel-filtration chromatography). Typically, this procedure yielded ∼3−4 mg of homogeneous protein (as assessed by SDS−PAGE) per liter of cell culture. The individual subunits (when expressed, purified separately, and subjected to urea treatment and rapid folding) did not have detectable activity (using **1**), but a mixture of subunits exhibited activity (data not shown). These observations indicate that the fully functional enzyme requires both subunits. The crystallography studies were conducted using the hh4-OT produced from the pET24a vector. All other experiments were conducted using hh4-OT (or the hh4-OT mutants) produced from the pBluescript construct.

The purified proteins were analyzed by electrospray ionization mass spectrometry (ESI-MS). The samples generate two major signals in the mass spectrometer. The α-subunit of wild type has a mass of 7730 Da, which corresponds to an expected 72-amino acid product with a calculated mass of 7732 Da. The β-subunit of

Table 2: Kinetic Parameters for 4-Oxalocrotonate Tautomerases Using 2-Hydroxymuconate (**1**)[a]

enzyme	k_{cat} (s^{-1})	K_m (μM)	k_{cat}/K_m (M^{-1} s^{-1})
hh4-OT[b]	3000 ± 100	70 ± 8	4.3×10^7
αR12A	43 ± 19	1033 ± 510	4.2×10^4
αR40A	65 ± 14	345 ± 100	1.9×10^5
βP1A	36 ± 1	17 ± 2	2.1×10^6
βR11A	3500 ± 100	69 ± 7	5.1×10^7
βR39A	733 ± 67	135 ± 27	5.4×10^6
4-OT	4000 ± 182	62 ± 8	6.5×10^7

[a]The steady-state kinetic parameters were determined in 10 mM potassium phosphate buffer (pH 7.3) at 24 °C. [b]Errors are standard deviations.

Table 3: Kinetic Parameters for 4-Oxalocrotonate Tautomerases Using Phenylenolpyruvate (**3**)[a]

enzyme	k_{cat} (s^{-1})	K_m (μM)	k_{cat}/K_m (M^{-1} s^{-1})
hh4-OT[b]	13 ± 1	121 ± 20	1.1×10^5
αR12A	0.6 ± 0.2	143 ± 80	4.2×10^3
αR40A	44 ± 8	152 ± 40	2.9×10^5
βP1A	0.2 ± 0.04	63 ± 22	3.2×10^3
βR11A	17 ± 3	198 ± 49	8.6×10^4
βR39A	11 ± 1	159 ± 24	7.0×10^4
4-OT	73 ± 6	199 ± 23	3.7×10^5

[a]The steady-state kinetic parameters were determined in 10 mM potassium phosphate buffer (pH 7.3) at 24 °C. [b]Errors are standard deviations.

the wild type has a mass of 7963 Da, which is 133 Da less than the calculated mass of 8096 Da (for a 73-amino acid product). The combined observations indicate that the β-subunit has undergone a post-translational modification for the removal of the initiating methionine whereas the α-subunit has not. The α- and β-subunits of the mutants show the same pattern (data provided in the Supporting Information). The initiating methionine is removed by a methionyl aminopeptidase, and the removal is correlated with the amino acid in the second position (*12*). Accordingly, in *E. coli*, a proline or alanine in position 2 (as seen in the β-subunit) results in a high likelihood of removal. However, if the second position is occupied by a leucine (as seen in the α-subunit), the likelihood of removal is very low (*12*).

Kinetic Characterization of Heterohexamer 4-OT. The kinetic parameters for hh4-OT were determined using 2-hydroxymuconate (**1**) and phenylenolpyruvate (**3**) and compared to those measured for the homohexamer 4-OT from *P. putida* (Tables 2 and 3). For both substrates, the K_m values are comparable whereas the k_{cat} values for the homohexamer 4-OT are slightly higher (1.3- and 6-fold higher using **1** and **3**, respectively) than those measured for hh4-OT. The higher k_{cat} values are reflected in higher k_{cat}/K_m values observed for the homohexamer 4-OT. The higher k_{cat} values may be due to the fact that hh4-OT is a thermophilic enzyme and is not operating at its optimum temperature.

The hh4-OT was also incubated separately with *trans*- and *cis*-3-chloroacrylic acid for 2 weeks. There was no change in the absorbance at 224 nm for either compound. Using this spectrophotometric assay, the hh4-OT does not appear to have low-level dehalogenase activity. The absence of activity (and the low extinction coefficient at 224 nm) prompted us to monitor an incubation mixture containing hh4-OT and **5** (Scheme 2) over a much longer time span by ^{1}H NMR spectroscopy. After 7 weeks, there was no spectral evidence of malonate semialdehyde (**6**), its hydrate, acetaldehyde, **7**, (resulting from nonenzymatic decarboxylation of **6**), or the hydrate of acetaldehyde.[4] (The enzyme still retains tautomerase activity using **1**.) In contrast, ~74% of compound **5** is converted to acetaldehyde and its hydrate in the presence of 4-OT (using approximately twice the amount of enzyme, 0.6 mg) in less than 6 days (*22*). Hence, there is no evidence of low-level CaaD activity comparable to that of 4-OT in the hh4-OT.

Kinetic Characterization of the hh4-OT Mutants. The importance of five residues (αArg-12[5], αArg-40, βPro-1, βArg-11, and βArg-39) to the hh4-OT activity was investigated by construction of the alanine mutants at each position and measurement of the kinetic parameters using **1** and **3** (Tables 2 and 3). The data show that replacing αArg-12, αArg-40, or βPro-1 with an alanine has significant effects on k_{cat} (using **1**), with 70-fold (αR12A), 46-fold (αR40A), and 83-fold (βP1A) decreases, respectively, being observed. There are increases in K_m for the αR12A and αR40A mutants (15- and 5-fold, respectively) and a small decrease in K_m for the βP1A mutant (4-fold). As a result, there are 1023-, 226-, and 20-fold decreases in k_{cat}/K_m for the αR12A, αR40A, and βP1A mutants, respectively. In contrast, replacing βArg-39 with an alanine has a small effect (4-fold decrease in k_{cat}, 2-fold increase in K_m, and 8-fold decrease in k_{cat}/K_m), and changing βArg-11 to an alanine has a negligible effect on the kinetic parameters. These results show that like 4-OT, two arginine residues (αArg-12 and αArg-40) and the amino-terminal proline (βPro-1) are required for the 1,5-enol-keto tautomerase activity using **1**.

With **3**, significant effects on the kinetic parameters are observed only for the αR12A and βP1A mutants. Replacing αArg-12 or βPro-1 with an alanine reduces k_{cat} 22- or 65-fold, respectively. The αR12A mutant shows little change in K_m, and the βP1A mutant shows a 2-fold decrease. The values of k_{cat}/K_m decrease 26-fold (αR12A) and 34-fold (βP1A). There is a small increase in k_{cat} for the αR40A mutant (3.4-fold) and little change in K_m. As a result, the k_{cat}/K_m increases 2.6-fold. There are smaller changes in the kinetic parameters for the βR11A and βR39A mutants. These results show that only αArg-12 and βPro-1 are required for the 1,3-enol-keto tautomerase activity using **3**.

Crystal Structure of hh4-OT. The crystal structure of hh4-OT was determined to confirm the oligomeric state and to explore the structural implications of the heterohexamer. Crystals of hh4-OT were grown using a precipitant solution of 0.25 M $(NH_4)_2SO_4$ and 4% PEG 4000 and diffracted to 2.41 Å. The structure was determined in a $P3_1$ space group using molecular replacement with a search model derived from a homology model of a theoretical hh4-OT based on a heterohexamer CaaD (PDB entry 1S0Y) scaffold (*25*), where the *H. influenzae* homologue (PDB entry 1MWW) and *Pseudomonas* sp. CF600 4-OT isozyme (PDB entry 1OTF) serve as templates for the α- and β-subunits, respectively (Table 1). The resulting hh4-OT structure consists of two heterohexamers per asymmetric unit.

Each heterohexamer contains three heterodimer units composed of one α-subunit and one β-subunit in an alternating fashion (Figure 2a). Both subunits have the signature 4-OT superfamily β−α−β scaffold, but the α-subunit displays one more β-sheet (encoded by residues Trp-51, Thr-52, and Val-53) than the β-subunit, which facilitates an α-subunit−α-subunit interaction (Figure 2b). Structural alignment of residues 2−50

[4]The nonenzymatic decarboxylation of malonate semialdehyde (**6**) yields acetaldehyde. Malonate semialdehyde is not sufficiently stable to accumulate in quantities that can be detected by ^{1}H NMR spectroscopy in the course of the lengthy incubation periods (*22*).

[5]The presence of the initiating methionine in the α-subunit increases the sequence number of each residue by one.

from each subunit of hh4-OT with the *Pseudomonas* sp. CF600 isozyme (PDB entry 1OTF) monomer resulted in a relatively low average rmsd of 1.5 Å. However, alignment of the α- and β-subunits of hh4-OT (using residues 2−50) has an average rmsd of 5.5 Å. The difference in rmsd can be attributed to the preceding and succeeding αA′ loops and the last 10 C-terminal residues of the selected alignment region (Figure 2c).

Active Site of hh4-OT. Two regions (designated "type I" and "type II") located at the interfaces of the three heterodimeric units could serve as potential active sites (Figure 2a). The three type I sites form around αMet-1, where the αAβ2 loop in the α-subunit, the β1′αA′ loop in the β-subunit, and a 3_{10} helix constitute the three sides of this region (Figure 3a). The type I site pocket is shallow, as it has been partially filled by αMet-1, and contains no arginine side chains. In addition, the αMet-1 side chain is inserted into a hydrophobic pocket where the hydroxyl group of βThr-52 forms a polar interaction with the sulfur atom of αMet-1. The βThr-52 position is typically occupied by a residue with a bulky hydrophobic side chain such as Phe-50, as seen in the *Pseudomonas* sp. CF600 and *P. putida* mt-2 4-OTs (*27*). However, the presence of such a residue in the β-subunit (and, in turn, at the active site) would clash with the side chain of αMet-1. The absence of Phe-50 is also one of the factors that facilitates the formation of a heterohexamer. The mutagenesis results (above) coupled with these structural observations eliminate the type I regions as active sites.

The three type II sites are formed at the other end of the heterodimeric unit interface around βPro-1 (Figure 3b). As with the type I sites, two of the type II active site sides are composed of loops, but these loops are contributed from different subunits, that is, the αA′β2′ loop in the β-subunit and the β1αA loop in the α-subunit. The third side of the type II active site is composed of the intramonomeric α-subunit β2−β3 loop instead of a 3_{10} helix (Figure 3b). The type II sites closely resemble the active sites in the *Pseudomonas* sp. CF600 and *P. putida* mt-2 4-OTs, as seen when the structures are overlaid (Figure 3a,c) (*27*). Within the type II sites, a positively charged hydrophilic pocket is created by three arginines, αArg-12, αArg-40, and βArg-39, as well as βThr-35. The general hydrophilic nature of this site allows it to be occupied by either one or two sulfates in the crystal structure. The mutagenesis results (above) and the sum of these structural observations identify the three type II regions as the active sites in the hh4-OT.

In addition to the charged and polar residues in the type II site, two hydrophobic pockets are created. One of these sites is created by the side chains of βPhe-29, βIle-33, and the side chain methyl group of βThr-35. The other pocket is formed by the side chains of αTrp-51 and αLeu-9. This second pocket is positioned in front of the prolyl nitrogen of βPro-1 suggesting that this pocket could reduce the pK_a of βPro-1 to that observed in the *P. putida* mt-2 4-OT (∼6.4) (*7*).

Thermostability of hh4-OT and 4-OT. Dynamic scanning calorimetry (DSC) was used to determine the melting temperatures (T_m) of hh4-OT and the homohexamer *P. putida* mt-2 4-OT (Figure 4a). The heat capacity for both samples was measured from 10 to 125 °C at 28 psi. Corrected for buffer effects, the T_m of the homohexamer *P. putida* mt-2 4-OT was found to be 78.8 °C, whereas the T_m of the heterohexamer *C. aurantiacus* 4-OT was 108.8 °C (Figure 4a). The observance of only one peak for hh4-OT suggests that the hexameric, dimeric, and secondary structure denatured at approximately the same temperature with no distinction between the α- and β-subunits. The higher T_m for

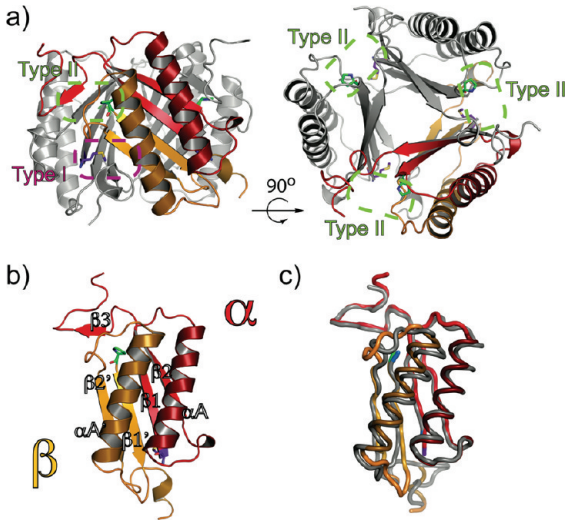

FIGURE 2: Structural composition of hh4-OT. (a) Biologically significant unit of hh4-OT viewed from the side and above. The α- and β-subunits of a heterodimer are colored red and orange, respectively, whereas the other two heterodimers are colored gray. The catalytic βPro-1 is colored green and αMet-1 purple. Additionally, type I (lavender) and type II (green) active sites are denoted as colored boxed regions superimposed onto hh4-OT. (b) Ribbon diagram of a single heterodimer using the colors defined above. (c) LSQKAB alignment of a single heterodimer of hh4-OT in the colors (defined above) superimposed on the *Pseudomonas* sp. CF600 4OT (PDB entry 1OTF), colored gray with the N-terminus colored blue.

the hh4-OT is likely a characteristic required for its stability in the thermophilic environment, and there is structural evidence that may explain the higher thermostability of the hh4-OT. The interactions between the α- and β-subunits of the hh4-OT are markedly more stable than those found in the homohexamer 4-OT. Specifically, these interactions are found in the core of the protein, where hh4-OT exhibits a unique set of three interdimer salt bridges between the α- and β-subunits, involving residues βGlu-4 and αArg-5 of each dimer. These salt bridges form a core for a network of hydrogen bonds involving the side chains of αGln-45, αThr-7, and αGln-44 (Figure 4b). Salt bridges have been shown previously to contribute significantly to the thermostability of an enzyme, both on the surface and in the protein core (*29*, *30*). These salt bridges also prohibit the formation of homohexamers composed of all α- or β-subunits. Such an arrangement would result in unfavorable electrostatic interactions between similarly negatively or positively charged amino acids, depending on the subunit. In contrast to hh4-OT's salt bridge core, the homohexamer 4-OT from *P. putida* mt-2 relies simply on water-mediated polar interactions among residues Thr-43, His-6, and Gln-4 (Figure 4c). The lack of intersubunit salt bridges in homohexamer 4-OT may be one factor that could impair its stability in a thermophilic environment.

DISCUSSION

The homohexamer 4-OT from *P. putida* mt-2 and *Pseudomonas* sp. CF600 has been extensively studied (*4*, *5*, *7*, *13*, *14*, *27*, *31*−*37*). The results of these studies identified key mechanistic and structural elements, delineated their roles, and produced a working hypothesis for the 4-OT mechanism (Scheme 3). In this mechanism, Pro-1 is a general base that abstracts the 2-hydroxyl proton (of **1**) for delivery to the C-5 position with a high degree of stereoselectivity (*31*−*33*). [In D_2O, the 5*S* isomer of [5-D]**2** is produced (*31*).] Pro-1 can function as a general base because the

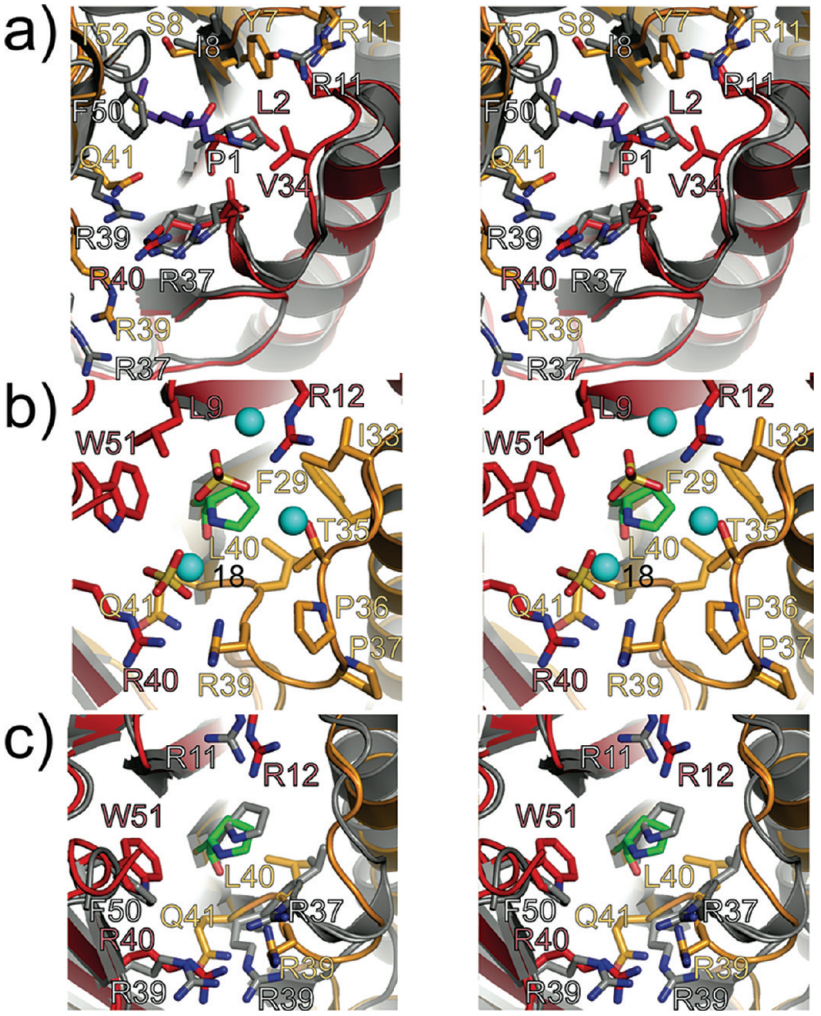

FIGURE 3: Active site of hh4-OT. (a) Divergent stereoview of the hh4-OT noncatalytic type I site formed by α-subunit E (red) and β-subunit D (orange), with αMet-1 colored purple. The active site of the *Pseudomonas* sp. CF600 4OT (PDB entry 1OTF) is superimposed in gray. (b) Divergent stereoview of the hh4-OT type II active site formed by α-subunit A (red) and β-subunit D (orange), with βPro-1 colored green. Water molecules are depicted as cyan spheres, and sulfate molecules are colored gold with pink oxygen molecules. (c) Divergent stereoview of the hh4-OT type II active site with *Pseudomonas* sp. CF600 4OT (PDB entry 1OTF) superimposed in gray.

prolyl nitrogen has a pK_a of ~6.4 so that it exists largely as the uncharged species at pH 7.3 (*33*). The side chains of three residues (Leu-8′, Met-45′, and Phe-50′)[6] constitute a hydrophobic pocket in front of the prolyl nitrogen and as such are likely the major groups responsible for the lowered pK_a of Pro-1 (*37*). In accord with this observation, changing Phe-50 to an alanine increases the pK_a of the prolyl nitrogen to 7.3, which is attributed to the increased solvent accessibility around Pro-1 (*37*). The remaining key catalytic residues are Arg-11 and Arg-39 (*14*, *35*, *36*). Arg-39 is proposed to interact with the 2-hydroxyl group (of **1**) and a C-1 carboxylate oxygen and has primarily a catalytic role. Arg-11 is proposed to interact with the C-6 carboxylate group in a bidentate fashion, which binds substrate and draws electron density away from C-5, thereby creating a partial positive charge at this position to facilitate protonation.

The structural homology, the positional conservation of key groups, and mutagenic results suggest that the hh4-OT mechanism parallels that of 4-OT. Accordingly, βPro-1 functions as the general base, and the two arginine residues, αArg-12[5] and αArg-40, interact with the C-6 and C-1 carboxylate groups, respectively. αArg-40 may also interact with the 2-hydroxyl group and stabilize the developing carbanion charge after its deprotonation. The pK_a of the βPro-1 is likely comparable to that of Pro-1 in 4-OT because of the hydrophobic pocket formed by αLeu-9 and αTrp-51 (comparable to Leu-8 and Phe-50, respectively, in *P. putida* mt-2 4-OT).

The results of the mutagenesis experiments with βPro-1, αArg-12, and αArg-40 are in accord with the proposed mechanism and parallel the results obtained for 4-OT. Thus, changing the rigid secondary amine (i.e., βPro-1) to a more flexible primary amine (i.e., βAla-1) primarily affects k_{cat} and k_{cat}/K_m. This observation suggests that the mutation affects the reaction chemistry, release of product, or both (*34*). The decreased activity could be due to a decrease in basicity coupled with a suboptimal positioning of the catalytic base due to the increased flexibility of the primary amine. The small decrease in K_m for the βP1A mutant may be due to the removal of bulk (e.g., the five-membered ring system), making binding more favorable (if K_m is a reflection of binding). It is not unexpected to see activity for the βP1A mutant because βAla-1 still has an amino-terminal group that can function as a base. Both the P1G and P1A mutants of 4-OT retain a significant amount of activity (*34*). Changing αArg-12 to an alanine affects both K_m and k_{cat}, consistent with its role in binding (C-6) and

[6]The primed residues refer to different subunits within the 4-OT homohexamer.

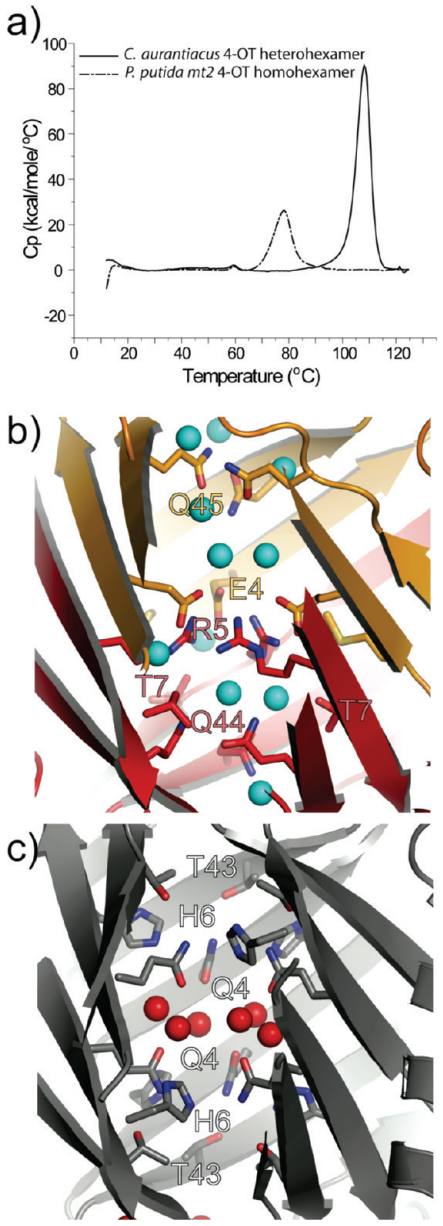

FIGURE 4: Thermostability of hh4-OT and 4-OT. (a) Thermal denaturation of *P. putida* mt-2 4-OT and hh4-OT at pH 7.3 by differential scanning calorimetry. Curves are derived from the average of five DSC scans per protein with the baseline subtracted. (b) Internal cavity of hh4-OT. The α- and *β*-subunits are colored red and orange, respectively. Water molecules are depicted as cyan spheres. (c) Internal cavity of 4-OT from *P. putida* mt-2 (PDB entry 4OTB) aligned as described for panel b. Waters are depicted as red spheres.

catalysis (drawing electron density away from C-5) (*7*, *35*, *36*). Changing αArg-40 to an alanine affects both K_m and k_{cat}, but the effect on K_m is not as severe as that seen for the αR12A mutant (*35*, *36*). Hence, the function of αArg-40 is predominantly catalytic.[7]. Both results are consistent with those observed for 4-OT mutants.

The behavior of hh4-OT and its mutants with the nonphysiological substrate **3**, a monoacid, implicates *β*Pro-1 and αArg-12 in catalysis. The reduced activity of the *β*P1A mutant can again be ascribed to a decrease in basicity along with a suboptimal positioning of the catalytic base, as discussed above. Changing

[7]The pK_a of Pro-1 in the R39Q mutant of 4-OT is 7.1 (*36*). A similar pK_a for Pro-1 in the αR40A mutant of hh4-OT could partially contribute to its decrease in activity.

Scheme 3

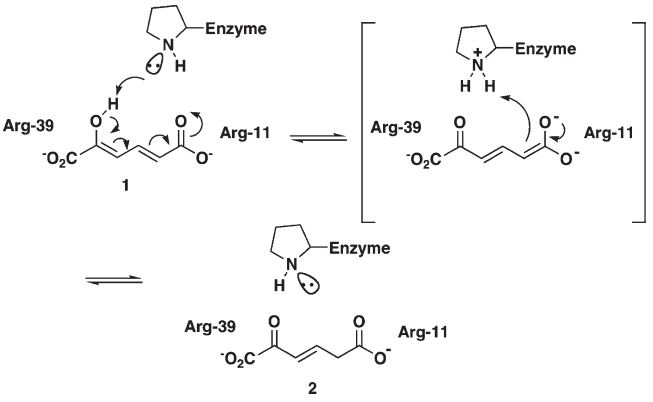

αArg-12 to an alanine affects k_{cat}, but not K_m. This observation argues against a binding role for αArg-12 and instead suggests a catalytic role. The absence of the positively charged arginine at this position could destabilize the developing carbanionic character of the intermediate after deprotonation of the 2-hydroxyl group. The mutation may also affect the pK_a of *β*Pro-1 or the positioning of a catalytic group or groups. The other arginine residues (αArg-40, *β*Arg-11, and *β*Arg-39) do not appear to be involved in binding or catalysis.

The results of modeling studies are consistent with the proposed orientations in the active site (Figure 5). Modeling **1** into the active site shows the respective interactions of the C-6 carboxylate and C-1 carboxylate groups with αArg-12 and αArg-40 (Figure 5a). *β*Pro-1 is proximal to the 2-hydroxyl proton. Modeling **3** into the active site shows the proximity of the C-1 carboxylate group to αArg-12 (Figure 5b). Again, *β*Pro-1 is near the 2-hydroxyl proton (of **3**). Candidates that might bind the C-1 carboxylate group were not identified, but the interaction between the phenyl ring of **3** and αTrp-51 is one possible binding determinant.

Stereochemical experiments could shed further light on the binding of **3**. For example, if the monoacid **3** binds in a single orientation (with the C-1 carboxylate end pointing toward αArg-12), then a high degree of stereoselectivity is expected (at C-3 of **4**) when the reaction is conducted in D_2O. If compound **3** binds in two orientations (the C-1 carboxylate end pointing toward αArg-12 or the C-1 carboxylate end pointing toward αArg-40), then a mixture of stereoisomers is expected.

The characterization of the two tautomerase sequences of *C. aurantiacus* J-10-fl and the conservation of key mechanistic and structural residues suggest that the gene products in the four other organisms (in Figure 1) will also form functional heterohexamers with 1,5- and 1,3-keto-enol tautomerase activities using **1** and **3**, respectively. These hh4-OTs are likely composed of three heterodimers, where each dimer consists of an α- and *β*-subunit. The heterohexamer structure presumably confers thermostability. Finally, *β*Pro-1, αArg-12, and *β*Arg-40 are present in these sequences and have roles analogous to those of *C. aurantiacus* hh4-OT.

Thus far, the only other characterized heterohexamer in the tautomerase superfamily is CaaD, which catalyzes the hydrolytic dehalogenation of *trans*-3-chloroacrylate [**5** (Scheme 2)] (*17*, *26*). Like the hh4-OT, CaaD is a trimer of dimers in which the three active sites are composed of residues from α- and *β*-subunits (*26*). Both subunits of CaaD have an amino-terminal proline, but only *β*Pro-1 is catalytic. Accordingly, the active site in one heterodimer is composed of *β*Pro-1, αArg-8, αArg-11, and αGlu-52 (Scheme 4).

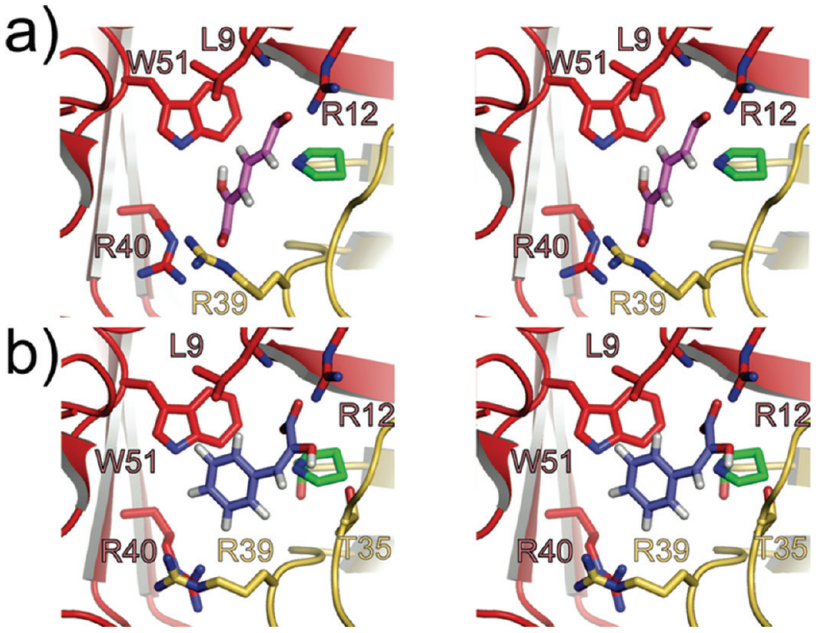

FIGURE 5: Comparison of hh4-OT substrate-bound models. (a) Divergent stereoview of the hh4-OT active site (PDB entry 3MB2) with 2-hydroxymuconate (pink) modeled in the site. β-Pro-1 is colored green, α-subunit A red, and β-subunit D orange. (b) Divergent stereoview of the hh4-OT active site with phenylenolpyruvate (purple) modeled in the site. All other atoms are shown as described in panel a.

Scheme 4

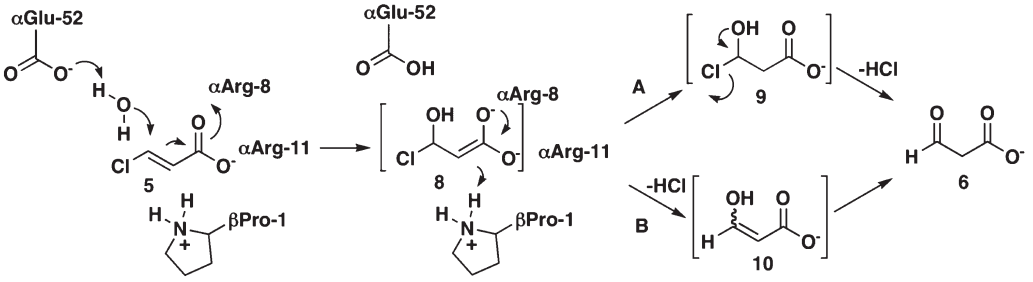

In the proposed mechanism, the arginine pair interacts with the carboxylate group of the substrate to bind and polarize the substrate, and αGlu-52 activates water for addition at C-3. These actions produce the enediolate species **8**, which can undergo two fates (route A or B) (*26*, *38*). In route A, βPro-1 provides a proton at C-2 and the resulting species **9** collapses to **6** by the direct expulsion of the chloride (*26*, *38*). In route B, rearrangement of **8** with the elimination of chloride (i.e., an α,β-elimination) yields enol **10**, which can tautomerize to **6** (*26*, *38*). Again, βPro-1 may provide a proton at C-2.

P. putida mt-2 4-OT has a low-level CaaD activity (as well as a low-level *cis*-CaaD activity) (*22*).[8] Mutagenic analysis implicated Pro-1 as a critical residue for the CaaD activity, but not Arg-11.[9] Hence, it was proposed that Arg-11 or Arg-39 interacted with the C-1 carboxylate group of the substrate, thereby polarizing the α,β-unsaturated acid and creating a partial positive charge at C-3 (Scheme 5). Water could then attack at C-3 with (or without) the assistance of Pro-1 (*22*). Further support for this mechanism came from the observation that changing Leu-8 in 4-OT to an arginine enhanced the low-level CaaD activity (*14*). The

Scheme 5

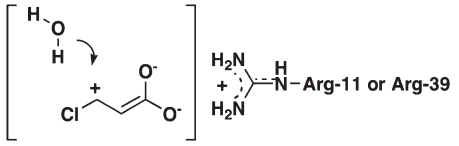

additional arginine is proposed to assist in polarization of the substrate and perhaps result in a preferred orientation of the substrate where the interaction with the two arginines is now favored over the interaction with a single arginine, Arg-39.

In contrast, hh4-OT does not have a low-level CaaD activity. This observation is particularly curious because of the striking similarities in the active sites, including the presence of the key residues associated with the low-level CaaD activity of 4-OT (i.e., βPro-1 and αArg-12). One possible explanation for the absent activity may reside with the presence of αTrp-51 instead of a phenylalanine, found in both CaaD (αPhe-50) and 4-OT (Phe-50). A comparison of the active sites suggests that the extra bulk of this residue in hh4-OT fills the cavity and may exclude an appropriately placed water molecule or interfere with the action of Pro-1. This observation implies that the other hh4-OTs identified in this study (i.e., Figure 1) will not have a low-level CaaD activity because tryptophan is conserved at this position.

[8]The *Pseudomonas* sp. CF600 4-OT has not been examined for low-level dehalogenase activity.

[9]Changing Arg-11 to an alanine increases the CaaD activity of 4-OT (*22*). Arg-39 presumably interacts with the carboxylate group of the substrate in the R11A 4-OT.

Although Phe-50 is critical for the tautomerase activity of 4-OT, this is the first indication that it may also be critical for the low-level CaaD activity (of 4-OT). Changing the phenylalanine to a tryptophan in 4-OT might diminish or eliminate the activity, whereas changing the tryptophan to a phenylalanine might introduce the activity in hh4-OT. Moreover, the newly introduced activity could be enhanced by the αL9R mutation (comparable to the L8R mutation of 4-OT). The effects of these mutations on the parent tautomerase activity are not known.

If the αW51F mutant of hh4-OT has measurable CaaD activity that is enhanced by additional mutagenesis, it would further support a scenario for the evolution of new enzymatic activities demonstrated by Gerlt and colleagues (*39*, *40*). It was found that a single mutation in L-Ala-D,L-Glu epimerase (AEE), an enolase superfamily member, introduced a low-level activity of another superfamily member, *o*-succinylbenzoate synthase (OSBS). Three additional mutations to the now functionally promiscuous construct produced an enzyme with a rate acceleration that was only 2 orders of magnitude slower than that of the natural *E. coli* OSBS. The improvement in activity was caused by an increase in substrate specificity. This sequence of events likely mimics (on some level) nature's process for generating new enzymatic activities; that is, a promiscuous enzyme is first created and then enhanced by a small number of mutations (*39*, *40*). The hh4-OT may likewise develop into an interesting model system for the exploration of the evolution of CaaD activity in the tautomerase superfamily. The appropriate experiments are underway.

ACKNOWLEDGMENT

We thank Dr. Michael T. Madigan for the generous gift of *C. aurantiacus* J-10-fl. The cells were grown in the laboratory of Dr. David Graham (Department of Chemistry and Biochemistry, The University of Texas). Supporting institutions of the SER-CAT 22-BM beamline at the Advanced Photon Source, Argonne National Laboratory, can be found at www.ser-cat.org/members.html.

SUPPORTING INFORMATION AVAILABLE

Expression, overproduction, and purification protocols for hh4-OT; experimental procedures used for the construction, expression, overproduction, purification, and mass spectral analysis of the hh4-OT mutants and the construction and expression of the separate subunits of the hh4-OT; and molecular modeling studies. This material is available free of charge via the Internet at http://pubs.acs.org.

REFERENCES

1. Harayama, S., Lehrbach, P. L., and Timmis, K. N. (1984) Transposon mutagenesis analysis of *meta*-cleavage pathway operon genes of the TOL plasmid of *Pseudomonas putida* mt-2. *J. Bacteriol. 160*, 251–255.
2. Harayama, S., Rekik, M., Ngai, K.-L., and Ornston, L. N. (1989) Physically associated enzymes produce and metabolize 2-hydroxy-2,4-dienoate, a chemically unstable intermediate formed in catechol metabolism via *meta* cleavage in *Pseudomonas putida*. *J. Bacteriol. 171*, 6251–6258.
3. Dagley, S. (1978) Pathways for the utilization of organic growth substrates. In The Bacteria: A Treatise on Structure and Function (Ornston, L. N., and Sokatch, J. R., Eds.) pp 305−388, Academic Press, New York.
4. Whitman, C. P., Aird, B. A., Gillespie, W. R., and Stolowich, N. J. (1991) Chemical and enzymatic ketonization of 2-hydroxymuconate, a conjugated enol. *J. Am. Chem. Soc. 113*, 3154–3162.
5. Wang, S. C., Johnson, W. H., Jr., Czerwinski, R. M., Stamps, S. L., and Whitman, C. P. (2007) Kinetic and stereochemical analysis of YwhB, a 4-oxalocrotonate tautomerase homologue in *Bacillus subtilis*: Mechanistic implications for the YwhB- and 4-oxalocrotonate tautomerase-catalyzed reactions. *Biochemistry 46*, 11919–11929.
6. Murzin, A. G. (1996) Structural classification of proteins: New superfamilies. *Curr. Opin. Struct. Biol. 6*, 386–394.
7. Whitman, C. P. (2002) The 4-oxalocrotonate tautomerase family of enzymes: How nature makes new enzymes using a β-α-β structural motif. *Arch. Biochem. Biophys. 402*, 1–13.
8. Poelarends, G. J., and Whitman, C. P. (2004) Evolution of enzymatic activity in the tautomerase superfamily: Mechanistic and structural studies of the 1,3-dichloropropene catabolic enzymes. *Bioorg. Chem. 32*, 376–392.
9. de Jong, R. M., Bazzacco, P., Poelarends, G. J., Johnson, W. H., Jr., Kim, Y.-J., Burks, E. A., Serrano, H., Thunnissen, A.-M. W. H., Whitman, C. P., and Dijkstra, B. W. (2007) Crystal structures of native and inactivated *cis*-3-chloroacrylic acid dehalogenase: Structural basis for substrate specificity and inactivation by (*R*)-oxirane-2-carboxylate. *J. Biol. Chem. 282*, 2440–2449.
10. Almrud, J. J., Poelarends, G. J., Johnson, W. H., Jr., Serrano, H., Hackert, M. L., and Whitman, C. P. (2005) Crystal structures of the wild-type, P1A mutant, and inactivated malonate semialdehyde decarboxylase: A structural basis for the decarboxylase and hydratase activities. *Biochemistry 44*, 14818–14827.
11. Almrud, J. J., Kern, A. D., Wang, S. C., Czerwinski, R. M., Johnson, W. H., Jr., Murzin, A. G., Hackert, M. L., and Whitman, C. P. (2002) The crystal structure of YdcE, a 4-oxalocrotonate tautomerase homologue from *Escherichia coli*, confirms the structural basis for oligomer diversity. *Biochemistry 41*, 12010–12024.
12. Hirel, P.-H., Schmitter, J.-M., Dessen, P., Fayat, G., and Blanquet, S. (1989) Extent of N-terminal methionine excision from *Escherichia coli* proteins is governed by the side-chain length of the penultimate amino acid. *Proc. Natl. Acad. Sci. U.S.A. 86*, 8247–8251.
13. Chen, L. H., Kenyon, G. L., Curtin, F., Harayama, S., Bembenek, M. E., Hajipour, G., and Whitman, C. P. (1992) 4-Oxalocrotonate tautomerase, an enzyme composed of 62 amino acid residues per monomer. *J. Biol. Chem. 267*, 17716–17721.
14. Poelarends, G. J., Almrud, J. J., Serrano, H., Darty, J. E., Johnson, W. H., Jr., Hackert, M. L., and Whitman, C. P. (2006) Evolution of enzymatic activity in the tautomerase superfamily: Mechanistic and structural consequences of the L8R mutation in 4-oxalocrotonate tautomerase. *Biochemistry 45*, 7700–7708.
15. Sambrook, J., Fritsch, E. F., and Maniatis, T. (1989) Molecular Cloning: A Laboratory Manual, 2nd ed., Cold Spring Harbor Laboratory Press, Plainview, NY.
16. Nübel, U., Bateson, M. M., Madigan, M. T., Kühl, M., and Ward, D. M. (2001) Diversity and distribution in hypersaline microbial mats of bacteria related to *Chloroflexus* spp. *Appl. Environ. Microb. 67*, 4365–4371.
17. Wang, S. C., Person, M. D., Johnson, W. H., Jr., and Whitman, C. P. (2003) Reactions of *trans*-3-chloroacrylic acid dehalogenase with acetylene substrates: Consequences of and evidence for a hydration reaction. *Biochemistry 42*, 8762–8773.
18. Waddell, W. J. (1956) A simple ultraviolet spectrophotometric method for the determination of protein. *J. Lab. Clin. Med. 48*, 311–314.
19. Laemmli, U. K. (1970) Cleavage of structural proteins during the assembly of the head of bacteriophage T4. *Nature 227*, 680–685.
20. Pospiech, A., and Neumann, B. (1995) A versatile quick-prep of genomic DNA from Gram-positive bacteria. *Trends Genet. 11*, 217–218.
21. Poelarends, G. J., Serrano, H., Person, M. D., Johnson, W. H., Jr., Murzin, A. G., and Whitman, C. P. (2004) Cloning, expression, and characterization of a *cis*-3-chloroacrylic acid dehalogenase: Insights into the mechanistic, structural, and evolutionary relationship between isomer-specific 3-chloroacrylic acid dehalogenases. *Biochemistry 43*, 759–772.
22. Wang, S. C., Johnson, W. H., Jr., and Whitman, C. P. (2003) The 4-oxalocrotonate tautomerase- and YwhB-catalyzed hydration of 3*E*-haloacrylates: Implications for evolution of new enzymatic activities. *J. Am. Chem. Soc. 125*, 14282–14283.
23. Otwinowski, Z., and Minor, W. (1997) Processing of X-ray diffraction data collected in oscillation mode. *Methods Enzymol. 276*, 307–326.
24. Collaborative Computational Project, Number 4 (1994) The CCP4 suite: Programs for protein crystallography. *Acta Crystallogr. D50*, 760–763.
25. Bates, P. A., Kelley, L. A., MacCallum, R. M., and Sternberg, M. J. (2001) Enhancement of protein modeling by human intervention in applying the automatic programs 3D-JIGSAW and 3D-PSSM. *Proteins* No. Suppl. 5, 39–46.
26. de Jong, R. M., Brugman, W., Poelarends, G. J., Whitman, C. P., and Dijkstra, B. W. (2004) The X-ray structure of *trans*-3-chloroacrylic

acid dehalogenase reveals a novel hydration mechanism in the tautomerase superfamily. *J. Biol. Chem. 279*, 11546–11552.
27. Subramanya, H. S., Roper, D. I., Dauter, Z., Dodson, E. J., Davies, G. J., Wilson, K. S., and Wigley, D. B. (1996) Enzymatic ketonization of 2-hydroxymuconate: Specificity and mechanism investigated by the crystal structures of two isomerases. *Biochemistry 35*, 792–802.
28. Emsley, P., and Cowtan, K. (2004) Coot: Model-building tools for molecular graphics. *Acta Crystallogr. D60*, 2126–2132.
29. Makhatadze, G. I., Loladze, V. V., Ermolenko, D. N., Chen, X., and Thomas, S. T. (2003) Contribution of surface salt bridges to protein stability: Guidelines for protein engineering. *J. Mol. Biol. 327*, 1135–1148.
30. Missimer, J. H., Steinmetz, M. O., Baron, R., Winkler, F. K., Kammerer, R. A., Daura, X., and van Gunsteren, W. F. (2007) Configurational entropy elucidates the role of salt-bridge networks in protein thermostability. *Protein Sci. 16*, 1349–1359.
31. Whitman, C. P., Hajipour, G., Watson, R. J., Johnson, W. H., Jr., Bembenek, M. E., and Stolowich, N. J. (1992) Stereospecific ketonization of 2-hydroxymuconate by 4-oxalocrotonate tautomerase and 5-(carboxymethyl)-2-hydroxymuconate isomerase. *J. Am. Chem. Soc. 114*, 10104–10110.
32. Stivers, J. T., Abeygunawardana, C., Mildvan, A. S., Hajipour, G., Whitman, C. P., and Chen, L. H. (1996) Catalytic role of the amino-terminal proline in 4-oxalocrotonate tautomerase: Affinity labeling and heteronuclear NMR studies. *Biochemistry 35*, 803–813.
33. Stivers, J. T., Abeygunawardana, C., Mildvan, A. S., Hajipour, G., and Whitman, C. P. (1996) 4-Oxalocrotonate tautomerase: pH dependences of catalysis and pK_a values of active site residues. *Biochemistry 35*, 814–823.
34. Czerwinski, R. M., Johnson, W. H., Jr., Whitman, C. P., Harris, T. K., Abeygunawardana, C., and Mildvan, A. S. (1997) Kinetic and structural effects of mutations of the catalytic amino-terminal proline in 4-oxalocrotonate tautomerase. *Biochemistry 36*, 14551–14560.
35. Harris, T. K., Czerwinski, R. M., Johnson, W. H., Jr., Legler, P. M., Abeygunawardana, C., Massiah, M. A., Stivers, J. T., Whitman, C. P., and Mildvan, A. S. (1999) Kinetic, stereochemical, and structural effects of mutations of the active site arginine residues in 4-oxalocrotonate tautomerase. *Biochemistry 38*, 12343–12357.
36. Czerwinski, R. M., Harris, T. K., Johnson, W. H., Jr., Legler, P. M., Stivers, J. T., Mildvan, A. S., and Whitman, C. P. (1999) Effects of mutations of the active site arginine residues in 4-oxalocrotonate tautomerase on the pK_a values of active site residues and on the pH dependence of catalysis. *Biochemistry 38*, 12358–12366.
37. Czerwinski, R. M., Harris, T. K., Massiah, M. A., Mildvan, A. S., and Whitman, C. P. (2001) The structural basis for the perturbed pK_a of the catalytic base in 4-oxalocrotonate tautomerase: Kinetic and structural effects of mutations of Phe-50. *Biochemistry 40*, 1984–1995.
38. Azurmendi, H. F., Wang, S. C., Massiah, M. A., Poelarends, G. J., Whitman, C. P., and Mildvan, A. S. (2004) The roles of active-site residues in the catalytic mechanism of *trans*-3-chloroacrylic acid dehalogenase: A kinetic, NMR, and mutational analysis. *Biochemistry 43*, 4082–4091.
39. Schmidt, D. M. Z., Mundorff, E. C., Dojka, M., Bermudez, E., Ness, J. E., Govindarajan, S., Babbitt, P. C., Minshull, J., and Gerlt, J. A. (2003) Evolution potential of $(\beta/\alpha)_8$-barrels: Functional promiscuity produced by single substitutions in the enolase superfamily. *Biochemistry 42*, 8387–8393.
40. Vick, J. E., Schmidt, D. M. Z., and Gerlt, J. A. (2005) Evolutionary potential of $(\beta/\alpha)_8$-barrels: In vitro enhancement of a "new" reaction in the enolase superfamily. *Biochemistry 44*, 11722–11729.
41. Kabsch, W., and Sander, C. (1983) Dictionary of protein secondary structure: Pattern recognition of hydrogen-bonded and geometrical features. *Biopolymers 22*, 2577–2637.